Applied and Computational Mechanics 10 (2016) 27–48

Applied and Computational Mechanics

Using Fourier and Taylor series expansion in semi-analytical deformation analysis of thick-walled isotropic and wound composite structures

L. Jiran[a,*], T. Mares[a]

[a] *Czech Technical University in Prague, Faculty of Mechanical Engineering 166 07 Praha 6, Technická 4, Czech Republic*

Received 18 August 2015; received in revised form 16 May 2016

Abstract

Thick-walled tubes made from isotropic and anisotropic materials are subjected to an internal pressure while the semi-analytical method is employed to investigate their elastic deformations. The contribution and novelty of this method is that it works universally for different loads, different boundary conditions, and different geometry of analyzed structures. Moreover, even when composite material is considered, the method requires no simplistic assumptions. The method uses a curvilinear tensor calculus and it works with the analytical expression of the total potential energy while the unknown displacement functions are approximated by using appropriate series expansion. Fourier and Taylor series expansion are involved into analysis in which they are tested and compared. The main potential of the proposed method is in analyses of wound composite structures when a simple description of the geometry is made in a curvilinear coordinate system while material properties are described in their inherent Cartesian coordinate system. Validations of the introduced semi-analytical method are performed by comparing results with those obtained from three-dimensional finite element analysis (FEA). Calculations with Fourier series expansion show noticeable disagreement with results from the finite element model because Fourier series expansion is not able to capture the course of radial deformation. Therefore, it can be used only for rough estimations of a shape after deformation. On the other hand, the semi-analytical method with Fourier Taylor series expansion works very well for both types of material. Its predictions of deformations are reliable and widely exploitable.

Keywords: thick-walled tube, wound composite structures, Fourier and Taylor series, semi-analytical method, deformation analysis, internal pressure

1. Introduction

Fibrous composites have inherent non-classical behavior including large torsional warping and coupled deformations emerging from the anisotropic nature of these materials. Detailed models of thin-walled and thick-walled composite parts are essential in order to fully apply special anisotropic effects of composite materials in design and applications. Therefore, a close attention is devoted to the possibilities of analytical or semi-analytical analyses of anisotropic structures.

A detailed review of deformation theories for anisotropic laminated beams is introduced and various theories are discussed (together with their merits and demerits) in [7]. An anisotropic tube under the pressure inside and outside was considered and a plane strain problem was solved in [5]. A systematic method (the state space approach) for analysis of laminated composite tubes subjected to uniform pressuring is described in [18].

*Corresponding author. Tel.: +420 775 234 309, e-mail: lukas.jiran@seznam.cz.

Mechanical properties of filament wound composite pipes have been studied under bending [1], transverse loading [2], axial compression [16], and internal pressure loading conditions [22]. The classical laminated-plate theory was used for a prediction of a stress and strain response of wound tubes and the optimal winding angle was searched [14]. Filament-wound shell structures under radial body force (due to rotation) and internal and external pressure are analytically tested in [19]. An analytical procedure dealing with thick-walled filament-wound sandwich pipes under internal pressure and thermomechanical loading was developed in [21].

Various semi-analytical methods and procedures were used in analysis of laminate composite structures, especially in the analysis of free vibration of beams. Commonly used procedures are based on the approximation of variables by Fourier series expansion in combination with some numerical discretization technique. Several examples of these studies can be found in [6, 13, 20] and [10].

Another field of application of semi-analytical methods is in the buckling analysis: a buckling of an imperfect isotropic elastic cylindrical shell under axial compression is investigated in [8], the critical buckling load is predicted in [3] where Fourier series expansion is used for representation of cylindrical pressure vessel imperfections. The linear buckling of laminate composite cones is studied in [15], a semi-analytical model for prediction of behavior (the linear and non-liner) of laminated composite cylinders and cones is presented and verified in [4].

In the past, many different methods have been developed, but their validity is often limited to one type of load and simple geometry of studied structures. It is useful and desirable to develop new methods for analyses of thick-walled filament wound composite structures with almost any geometry that works universally for different types of load without simplistic assumptions.

2. Isotropic Tube under Internal Pressure

In the first part of this article, a simple isotropic tube under internal pressure load is used for the method description. This basic analysis is rather distant from the main purpose of the developed semi-analytical method, which itself is far from analyses of composite structures with complicated geometry, but an isotropic material allows a clear and simple definition of material properties in this method as well as in the finite element model that is used for results verification. Clear material properties definition and a simple shape enable us to focus the main attention on the method procedure and its verification.

2.1. Structure Description, Metric Tensors, Transformation Matrices

The tube is fixed at its both ends and three coordinate systems are introduced for its description: global Cartesian coordinate system x^i, local Cartesian coordinate system μ^i, see Fig. 2, Fig. 1, and global circular coordinate system ξ^i.

The major advantage of the semi-analytical method is in the description of the structure by using these two coordinate systems: x^i, ξ^i. Global circular coordinate system ξ^i is used as global computational coordinate system and whole deformation analysis is performed in this coordinate system because it allows a very practical description of the tube geometry. The semi-analytical analysis requires using of numerical integrations over the structure volume and it is very useful to perform these integrations in circular system ξ^i because it provides clear and simple limits of integrations. When coordinates ξ^i of global circular coordinate are used, the tube geometry is described by simple ranges

$$\xi^1 \in [0, t], \qquad \xi^2 \in [0, 2\pi], \qquad \xi^3 \in [0, l].$$

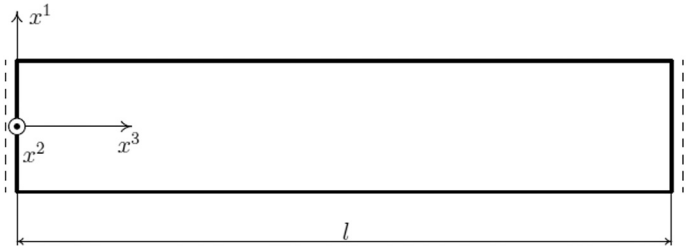

Fig. 1. Tube under internal pressure, boundary conditions

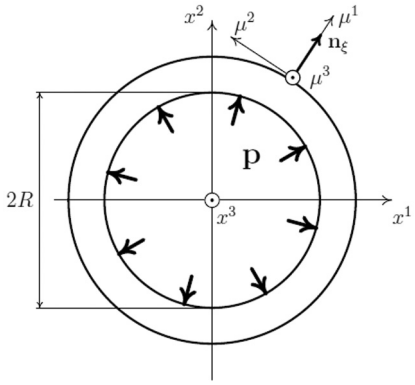

Fig. 2. Coordinate systems

Global Cartesian coordinate system x^i is natural for a human perception and it is commonly used for geometry representations and results plotting. Coordinate system x^i is also used for description of material properties. Relations for the transformation between these two coordinate systems (ξ^i and x^i) are known and therefore it is possible to take advantage of both coordinate systems in the computational procedure.

Relations between global circular coordinate system ξ^i and global Cartesian coordinate system x^i are

$$\begin{aligned} x^1 &= (R + \xi^1)\cos\xi^2, \\ x^2 &= (R + \xi^1)\sin\xi^2, \\ x^3 &= \xi^3, \end{aligned} \tag{1}$$

where R is inner diameter of the tube.

It is necessary to introduce metric tensors of all coordinate systems for analysis purposes. Simple notations are used for a clarity in the labeling: metric tensor of global Cartesian coordinate system x^i is denoted $\overset{x}{g}_{ij}$ and metric tensor of global cylindrical coordinate system ξ^i is denoted $\overset{\xi}{g}_{ij}$.

Coordinate system x^i is Cartesian and, due to this fact, we have for components of its metric tensor

$$\overset{x}{g}_{ij} = \delta_{ij}, \tag{2}$$

where δ_{ij} is the Kronecker delta.

Components of metric tensor $\overset{\xi}{g}_{ij}$ can be expressed via the transformation rule

$$\overset{\xi}{g}_{ij} = \frac{\partial x^k}{\partial \xi^i} \frac{\partial x^l}{\partial \xi^j} \overset{x}{g}_{kl}, \tag{3}$$

where components of metric tensor $\overset{x}{g}_{ij}$ are known from formula (2) and transformation matrix

$$\frac{\partial x^i}{\partial \xi^j} = \begin{pmatrix} \cos\xi^2 & -(R+\xi^1)\sin\xi^2 & 0 \\ \sin\xi^2 & (R+\xi^1)\cos\xi^2 & 0 \\ 0 & 0 & 1 \end{pmatrix}. \tag{4}$$

These forms imply

$$\overset{\xi}{g}_{ij} = \begin{pmatrix} 1 & 0 & 0 \\ 0 & (R+\xi^1)^2 & 0 \\ 0 & 0 & 1 \end{pmatrix}. \tag{5}$$

2.2. Deformation Analysis, Procedure Description

Deformations of the tube are determined by using the commonly known principle of the total potential energy minimum [11]. Total potential energy of the structure $\Pi(\overset{\xi}{u}_i)$ is expressed in the form

$$\Pi(\overset{\xi}{u}_i) = U(\overset{\xi}{u}_i) - W(\overset{\xi}{u}_i), \tag{6}$$

where $U(\overset{\xi}{u}_i)$ is elastic strain energy, $-W(\overset{\xi}{u}_i)$ is potential energy of applied forces, and $\overset{\xi}{u}_i$ are unknown displacement functions in global computational coordinate system ξ^i.

There are many possibilities how to approximate these unknown displacement functions by using a series expansion. In this paper, Fourier series with a complex exponentials basis and a combination of Fourier and Taylor series are employed in computational procedures. It is appropriate to mention a general comparison between Fourier series and Taylor series and also to briefly discuss their main advantages and restrictions.

A function is needed to be infinitely differentiable and then it is possible to approximate it by Taylor series. This restriction can be reduced when Taylor's theorem with a remainder is employed. Then the function must be differentiable only a finite number of times. Both conditions usually imply that the function must be continuous and therefore discontinuous functions cannot be represented by Taylor series expansion [9].

Fourier series offers possibility of representation of continuous functions but also of discontinuous functions because the only requirement on properties of the function is its integrability. The Fourier coefficients can be computed even for piecewise continuous functions but it is well known that in points of discontinuity a behavior of Fourier series differs from the function itself [9]. Behavior of Fourier series near these points of discontinuity is known as Gibbs' phenomenon. It describes that near points of discontinuity there is always an error in the form of an overshoot (about 9 % of the discontinuity) and it occurs independently of the number of terms in Fourier series [17].

The second important feature of Fourier series is that this series is highly valued in solving oscillatory problems.

In this present analysis, unknown displacement functions $\overset{\xi}{u}_i$ are approximated by Fourier series expansion. Fourier series expansion has to fulfil chosen boundary conditions i.e. that both tube bases ($x^3 = \xi^3 = 0$ and $x^3 = \xi^3 = l$) are fixed in all three directions, see Fig. 1.

Series fulfilling these boundary conditions has the form

$$\begin{aligned}
\overset{\xi}{u}_1 &= \sum_{hkm=-P}^{P} A_1^{hkm} \mathrm{e}^{\mathrm{i}h2\pi\xi^1} \mathrm{e}^{\mathrm{i}k\xi^2} \mathrm{e}^{\mathrm{i}m\xi^3\frac{2\pi}{l}} \xi^3(\xi^3 - l), \\
\overset{\xi}{u}_2 &= \sum_{hkm=-P}^{P} A_2^{hkm} \mathrm{e}^{\mathrm{i}h2\pi\xi^1} \mathrm{e}^{\mathrm{i}k\xi^2} \mathrm{e}^{\mathrm{i}m\xi^3\frac{2\pi}{l}} \xi^3(\xi^3 - l), \\
\overset{\xi}{u}_3 &= \sum_{hkm=-P}^{P} A_3^{hkm} \mathrm{e}^{\mathrm{i}h2\pi\xi^1} \mathrm{e}^{\mathrm{i}k\xi^2} \mathrm{e}^{\mathrm{i}m\xi^3\frac{2\pi}{l}} \xi^3(\xi^3 - l),
\end{aligned} \tag{7}$$

where A_1^{hkm}, A_2^{hkm}, A_3^{hkm} are coefficients to be determined. In (7), classical Fourier series expansion in the complex form is multiplied by coordinate ξ^3 and $(\xi^3 - l)$ in order to ensure fixation of both tube ends. All three displacement functions $\overset{\xi}{u}_1$, $\overset{\xi}{u}_2$, $\overset{\xi}{u}_3$ are equal to zero for all points at both tube bases where $x^3 = \xi^3 = 0$ and $x^3 = \xi^3 = l$. Parameter P in (7) determines the number of members of Fourier series expansion and is ideally equal to ∞. Three real possible values of this parameter ($P = 2, 3$, and 5, respectively) are tested in the analysis. Parameter P is chosen 3 for purpose of the following procedure description so that each displacement function is approximated by 7^3 members of Fourier series expansion.

The semi-analytical method with Fourier series expansion can be hereafter abbreviated for simplicity to SAF.

2.2.1. Inclusion of other Boundary Conditions

This paper presents only one type of boundary conditions but it should be mentioned that the semi-analytical method is highly effective in possibilities to include various types of boundary conditions.

The previous section shows how boundary conditions can be included directly to the series expansion. This process enables a simple fixation of whole cross sections in selected directions but also fixation of only selected points of the structure.

For example, following conditions are specified: whole left base ($x^3 = \xi^3 = 0$) is fixed in $\overset{\xi}{u}_3$ direction, point $A = [\xi^1_{(A)}, \xi^2_{(A)}, \xi^3_{(A)}] = [t, \pi, 0]$ is moreover fixed in the $\overset{\xi}{u}_2$ direction and point $B = [\xi^1_{(B)}, \xi^2_{(B)}, \xi^3_{(B)}] = [t, 0, 0]$ is fixed in all three directions.

Fourier series fulfilling these boundary conditions has the form

$$\begin{aligned}
\overset{\xi}{u}_1 &= \sum_{hkm=-P}^{P} A_1^{hkm} \mathrm{e}^{\mathrm{i}h2\pi\xi^1} \mathrm{e}^{\mathrm{i}k\xi^2} \mathrm{e}^{\mathrm{i}m\xi^3\frac{2\pi}{l}} \Big(\underbrace{\xi^3}_{(a)} + \underbrace{\sin^2\frac{\xi^2}{2}}_{(b)} + \underbrace{(t - \xi^1)}_{(c)} \Big), \\
\overset{\xi}{u}_2 &= \sum_{hkm=-P}^{P} A_2^{hkm} \mathrm{e}^{\mathrm{i}h2\pi\xi^1} \mathrm{e}^{\mathrm{i}k\xi^2} \mathrm{e}^{\mathrm{i}m\xi^3\frac{2\pi}{l}} \Big(\xi^3 + \underbrace{\sin^2\xi^2}_{(d)} + (t - \xi^1) \Big), \\
\overset{\xi}{u}_3 &= \sum_{hkm=-P}^{P} A_3^{hkm} \mathrm{e}^{\mathrm{i}h2\pi\xi^1} \mathrm{e}^{\mathrm{i}k\xi^2} \mathrm{e}^{\mathrm{i}m\xi^3\frac{2\pi}{l}} \xi^3,
\end{aligned} \tag{8}$$

where classical Fourier series in the complex form is multiplied by terms (a), (b), (c), and (d), respectively, and these terms have following meanings: term (a) is zero for all points of the left

base where coordinate $\xi^3 = 0$. Due to the fact that coordinate $\xi^2 \in [0, 2\pi]$, term (b) is equal to zero only when $\xi^2 = 0$ (point B). Term (d) vanishes when $\xi^2 = 0$ or $\xi^2 = \pi$ (points B and A). Similarly, term (c) is equal to zero for all points with coordinate $\xi^1 = t$.

The method of Lagrange multipliers is the second way to fulfil boundary conditions. This method is advantageous particularly in cases when specific boundary conditions are required. When the Lagrange multipliers are used, the analysis procedure is fairly changed and other matrices are involved into calculation.

2.2.2. Elastic energy

Elastic energy of the structure $U(\overset{\xi}{u}_i)$ in (6) is expressed as

$$\overset{\xi}{U} = \frac{1}{2} \int\limits_{\overset{\xi}{\Omega}} \overset{\xi}{E}{}^{ijkl}_{iso} \overset{\xi}{\varepsilon}_{ij} \overset{\xi}{\varepsilon}_{kl} \, \mathrm{d}\overset{\xi}{\Omega}, \tag{9}$$

where $\overset{\xi}{E}{}^{ijkl}_{iso}$ is elasticity tensor in global computational coordinate system and ε_{ij} is small strain tensor.

By using well known relations of continuum mechanics, elastic energy (9) can be written in the form that allows easy transition to the notation for numeric solution

$$\overset{\xi}{U} = \frac{1}{2} \int\limits_{\overset{\eta}{\Omega}} \left(\frac{\partial \overset{\xi}{u}_j}{\partial \xi^i} - \overset{\xi}{\Gamma}{}^a_{ij} \overset{\xi}{u}_a \right) \overset{\xi}{E}{}^{ijkl}_{iso} \left(\frac{\partial \overset{\xi}{u}_l}{\partial \xi^k} - \overset{\xi}{\Gamma}{}^a_{kl} \overset{\xi}{u}_a \right) \left| \overset{\xi}{g}_{ij} \right|^{\frac{1}{2}} \mathrm{d}\xi^1 \, \mathrm{d}\xi^2 \, \mathrm{d}\xi^3, \tag{10}$$

where Γ^k_{ij} are Christoffel symbols of the second kind.

Elastic energy (10) can be transformed to the form usable for the numerical solution. Partial derivatives in (10) can be written in the following way

$$\left\{ \frac{\partial \overset{\xi}{u}_i}{\partial \xi^j} \right\}_{ij\lceil_{[9,1]}} = B_{[9,1\,029]} A_{[1\,029,1]}, \tag{11}$$

where symbol $ij\lceil$ indicates how the items are stored in column vector and $[9, 1]$, $[9, 1\,029]$, or $[1\,029, 1]$ indicate matrices and vectors dimensions for 7^3 members of Fourier series. Matrix B reads[1]

$$B = \begin{pmatrix} \partial v_1/\partial \xi^1 & \mathtt{zeros}(1,343) & \mathtt{zeros}(1,343) \\ \partial v_1/\partial \xi^2 & \mathtt{zeros}(1,343) & \mathtt{zeros}(1,343) \\ \partial v_1/\partial \xi^2 & \mathtt{zeros}(1,343) & \mathtt{zeros}(1,343) \\ \mathtt{zeros}(1,343) & \partial v_2/\partial \xi^1 & \mathtt{zeros}(1,343) \\ \mathtt{zeros}(1,343) & \partial v_2/\partial \xi^2 & \mathtt{zeros}(1,343) \\ \mathtt{zeros}(1,343) & \partial v_2/\partial \xi^3 & \mathtt{zeros}(1,343) \\ \mathtt{zeros}(1,343) & \mathtt{zeros}(1,343) & \partial v_3/\partial \xi^1 \\ \mathtt{zeros}(1,343) & \mathtt{zeros}(1,343) & \partial v_3/\partial \xi^2 \\ \mathtt{zeros}(1,343) & \mathtt{zeros}(1,343) & \partial v_3/\partial \xi^3 \end{pmatrix}, \tag{12}$$

[1]Typewrite font is used for the MATLAB syntax.

where displacement functions are expressed

$$\overset{\xi}{u}_i = N_{[3,1\,029]} A_{[1\,029,1]}, \tag{13}$$

with new matrix

$$N = \begin{pmatrix} v_1 & \texttt{zeros}(1,343) & \texttt{zeros}(1,343) \\ \texttt{zeros}(1,343) & v_2 & \texttt{zeros}(1,343) \\ \texttt{zeros}(1,343) & \texttt{zeros}(1,343) & v_3 \end{pmatrix}, \tag{14}$$

where

$$v_1 = v_2 = v_3 = \mathrm{e}^{\mathrm{i}h2\pi\xi^1} \mathrm{e}^{\mathrm{i}k\xi^2} \mathrm{e}^{\mathrm{i}m\xi^3 \frac{2\pi}{l}} \xi^3(\xi^3 - l). \tag{15}$$

Notation $\texttt{zeros}(1,343)$ in terms (12) and (14) represents the MATLAB command to create array of all zeros of desired dimensions (e.g., 1 row and 343 columns in this particular case).

Column vector of coefficients to be determined in (11) is

$$A = \begin{pmatrix} A_1^{hkm} \\ A_2^{hkm} \\ A_3^{hkm} \end{pmatrix}. \tag{16}$$

Using matrices A and B, we can express

$$\left(\frac{\partial \overset{\xi}{u}_j}{\partial \xi^i} - \overset{\xi}{\Gamma}{}^a_{ij} \overset{\xi}{u}_a \right) = \left(B_{[9,1\,029]} - G_{[9,1\,029]} \right) A_{[1\,029,1]}, \tag{17}$$

where

$$G = \left\{ \overset{\xi}{\Gamma}{}^1_{ij} \right\}_{ij\lceil} (v_1 \ \texttt{zeros}(1,343) \ \texttt{zeros}(1,343)) + \left\{ \overset{\xi}{\Gamma}{}^2_{ij} \right\}_{ij\lceil} (\texttt{zeros}(1,343) \ v_2 \ \texttt{zeros}(1,343)). \tag{18}$$

Term (18) does not include $\overset{\xi}{\Gamma}{}^3_{ij}$ because $\overset{\xi}{\Gamma}{}^3_{ij} = 0$ for this presented case.

Finally, elastic energy (10) can be written as

$$\overset{\xi}{U} = \frac{1}{2} A^{\mathrm{T}} \overset{\xi}{K} A, \tag{19}$$

where $\overset{\xi}{K}$ is stiffness matrix of the structure

$$\overset{\xi}{K} = \int_0^l \int_0^{2\pi} \int_0^t (B-G)^{\mathrm{T}} \overset{\xi}{E}{}^{ijkl}_{iso} (B-G) \left| \overset{\xi}{g}_{ij} \right|^{\frac{1}{2}} \mathrm{d}\xi^1 \, \mathrm{d}\xi^2 \, \mathrm{d}\xi^3. \tag{20}$$

2.2.3. Elasticity Tensor

Elasticity tensor of the isotropic material $\overset{x}{E}{}^{ijkl}_{iso}$ is known in global Cartesian coordinate system x^i and has to be transformed into global computational coordinate system ξ^i according to the rule

$$\overset{\xi}{E}{}^{ijkl}_{iso} = \frac{\partial \xi^i}{\partial x^m}\frac{\partial \xi^j}{\partial x^n}\frac{\partial \xi^k}{\partial x^o}\frac{\partial \xi^l}{\partial x^p}\ \overset{x}{E}{}^{mnop}_{iso}, \tag{21}$$

with the transformation matrix given by the inversion of (4). It is possible to express $\overset{x}{E}{}^{ijkl}_{iso}$ in the form for the numerical solution

$$\texttt{Exi} = \texttt{kron}(\texttt{xix}, \texttt{xix}) * \texttt{Ex} * \texttt{kron}(\texttt{xix.}', \texttt{xix.}'), \tag{22}$$

where `xix` denotes inversion of transformation matrix (4) and `kron` is the MATLAB command that returns the Kronecker tensor product of matrices `xix`.

In the case of the isotropic material, elasticity tensor `Ex` is used in the form

$$\texttt{Ex} = \begin{pmatrix} \alpha & 0 & 0 & 0 & \beta & 0 & 0 & 0 & \beta \\ 0 & \gamma & 0 & \gamma & 0 & 0 & 0 & 0 & 0 \\ 0 & 0 & \gamma & 0 & 0 & 0 & \gamma & 0 & 0 \\ 0 & \gamma & 0 & \gamma & 0 & 0 & 0 & 0 & 0 \\ \beta & 0 & 0 & 0 & \alpha & 0 & 0 & 0 & \beta \\ 0 & 0 & 0 & 0 & 0 & \gamma & 0 & \gamma & 0 \\ 0 & 0 & \gamma & 0 & 0 & 0 & \gamma & 0 & 0 \\ 0 & 0 & 0 & 0 & 0 & \gamma & 0 & \gamma & 0 \\ \beta & 0 & 0 & 0 & \beta & 0 & 0 & 0 & \alpha \end{pmatrix}, \tag{23}$$

where

$$\alpha = \frac{E(\nu^2-1)}{2\nu^3+3\nu^2-1}, \quad \beta = -\frac{E(\nu^2+\nu)}{2\nu^3+3\nu^2-1}, \quad \gamma = G$$

with engineering constants: E, ν, G, (Young's modulus, Poisson's ratio, and shear modulus of the chosen material, respectively).

2.2.4. Work of Applied Forces

The tube is loaded by internal pressure p, see Fig. 2, and work done by this pressure on the inner face can be written as

$$\overset{\xi}{W} = \overset{\xi}{P}\ A, \tag{24}$$

where A is column vector of coefficients, see (16).

Load vector for Fourier series expansion

$$\overset{\xi}{P} = \int_0^l \int_0^{2\pi} p\ \overset{\xi}{n^i}{}^{\mathrm{T}}\ N \left| \overset{\xi}{a}_{ij} \right|^{\frac{1}{2}}\ \mathrm{d}\xi^3\, \mathrm{d}\xi^2, \tag{25}$$

where N is defined by form (14) and $\overset{\xi}{n^i}$ is outer normal of the circle in global computational coordinate system ξ^i

$$\overset{\xi}{n^i} = \frac{\partial \xi^i}{\partial x^k}\frac{\partial x^k}{\partial \mu^m}\ \overset{\mu}{n^m}, \tag{26}$$

where

$$\overset{\mu}{n}{}^{i} = \begin{pmatrix} 1 \\ 0 \\ 0 \end{pmatrix} \tag{27}$$

is outer normal of the circle in coordinate system μ^i, see Fig. 2.

Components $\overset{\xi}{a}_{ij}$ in (25) are components of metric tensor in computational coordinate system with fixed radius

$$\overset{\xi}{a}_{ij} = \begin{pmatrix} \overset{\xi}{g}_{22} & \overset{\xi}{g}_{23} \\ \overset{\xi}{g}_{23} & \overset{\xi}{g}_{33} \end{pmatrix} = \begin{pmatrix} \overset{\xi}{g}_{22} & 0 \\ 0 & 1 \end{pmatrix}. \tag{28}$$

Transformation matrix between coordinate systems x^i, μ^i in term (26) is

$$\frac{\partial x^i}{\partial \mu^j} = \begin{pmatrix} n^1_\xi & -n^2_\xi & 0 \\ n^2_\xi & n^1_\xi & 0 \\ 0 & 0 & 1 \end{pmatrix}, \tag{29}$$

with

$$n^1_\xi = \frac{\frac{\partial x^2}{\partial \xi^2}}{\sqrt{\left(\frac{\partial x^1}{\partial \xi^2}\right)^2 + \left(\frac{\partial x^2}{\partial \xi^2}\right)^2}} = \cos\xi^2, \quad n^2_\xi = \frac{-\frac{\partial x^1}{\partial \xi^2}}{\sqrt{\left(\frac{\partial x^1}{\partial \xi^2}\right)^2 + \left(\frac{\partial x^2}{\partial \xi^2}\right)^2}} = \sin\xi^2,$$

where $\mathbf{n}_\xi = (n^1_\xi, n^2_\xi, 0)$ is outer normal to the circle, see Fig. 2.

Form (25) clearly demonstrates that it is very simple to include different courses of an internal pressure into the semi-analytical method. The internal pressure may vary according to length coordinate ξ^3 or circumferential coordinate ξ^2 or according both coordinates together. However, this paper deals with the semi-analytical method verification and only loading by constant internal pressure is used for this purpose.

2.2.5. Displacement Functions

Total potential energy is expressed by form (6). When we use elastic energy in form (19) and work of the applied force in form (24), we can write for total potential energy

$$\overset{\xi}{\Pi} = \frac{1}{2} A^{\mathrm{T}} \overset{\xi}{K} A - \overset{\xi}{P} A. \tag{30}$$

The necessary condition of the minimum of total potential energy

$$\frac{\partial \overset{\xi}{\Pi}}{\partial A} = 0 \tag{31}$$

leads to column vector of coefficients to be determined

$$A = \overset{\xi}{K}{}^{-1} \overset{\xi}{P}. \tag{32}$$

Displacement functions in global computational coordinate system

$$\begin{pmatrix} \overset{\xi}{u}_1 \\ \overset{\xi}{u}_2 \\ \overset{\xi}{u}_3 \end{pmatrix} = \texttt{real}(\texttt{N} * \texttt{A}), \tag{33}$$

where `real` is the MATLAB command that returns the real part of the elements of the complex matrix. Matrix N in (33) is defined by (14). We can express and plot these functions in global Cartesian coordinate system x^i

$$\overset{x}{u}_j = \frac{\partial \xi^i}{\partial x^j} \overset{\xi}{u}_i \,. \tag{34}$$

Thus it is possible to determine displacement functions of any point of the structure.

2.2.6. Results

The analysis of radial deformations in isotropic thick-walled cylindrical vessels submitted to the action of internal pressure can be performed analytically for some basic cases.

The thick-walled open pressure vessel loaded by internal pressure p is considered and its radial deformations are computed. Radial deformations in the middle of the tube length (i.e. away from the ends of the tube where the deformations are not affected by edge effects) can be calculated according to the formula

$$\Delta r_{(x^2)} = \frac{x^2}{E}\left(K(1-\nu) + \frac{C}{(x^2)^2}(1+\nu)\right), \tag{35}$$

where constants

$$K = \frac{pR^2}{(R+t)^2 - R^2}, \quad C = \frac{pR^2(R+t)^2}{(R+t)^2 - R^2}.$$

It is obvious from (35) that the course of radial deformation through the wall thickness has the form of a hyperbolic function and the question is how Fourier series expansion is able to approximate this hyperbolic course.

Results obtained by using the semi-analytical method with Fourier series expansion are presented and compared with the FEM results in two separate figures where radial deformations through the wall thickness (in the middle of the tube length: $x^3 = l/2$) and radial deformations of the outer face through the tube length are plotted, see Fig. 3, Fig. 4.

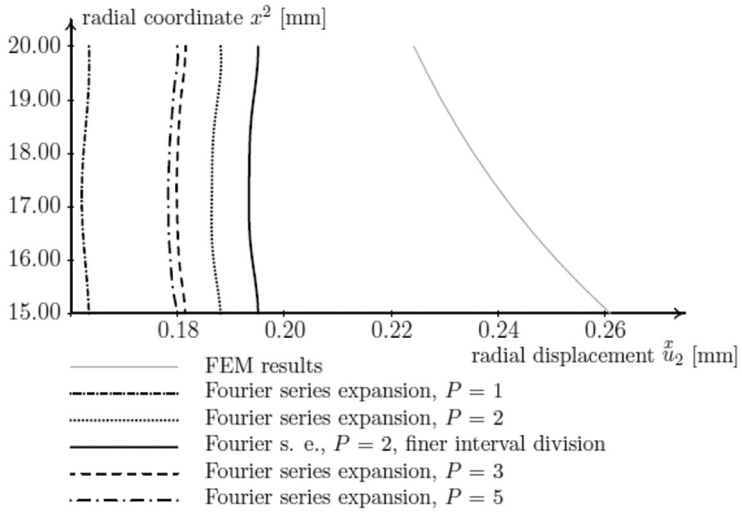

Fig. 3. Course of radial deformation evaluated at longitudinal coordinate $x^3 = l/2$, Fourier series expansion

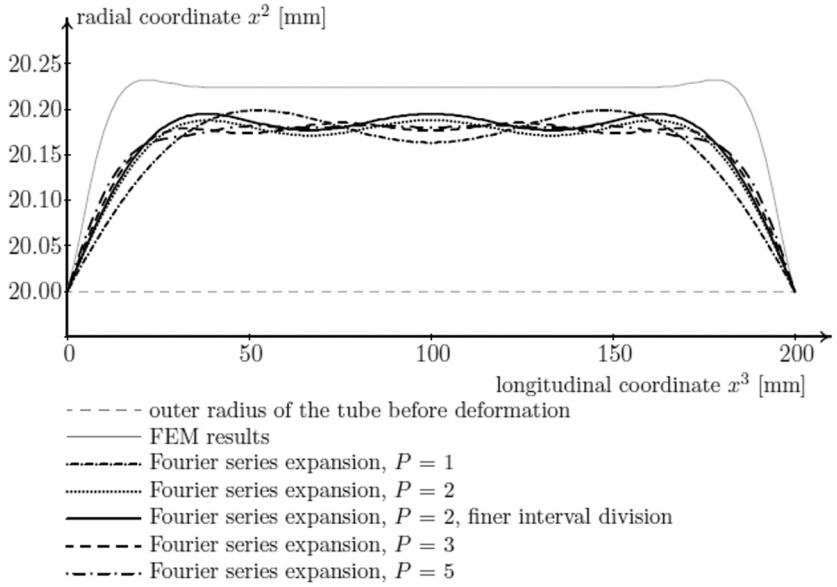

Fig. 4. Course of the outer face deformation, Fourier series expansion

Numerical results are presented for the following input values:

$$R = 15\ [\mathrm{mm}],\ t = 5\ [\mathrm{mm}],\ l = 200\ [\mathrm{mm}],\ \nu = 0.3,\ E = 210\,000\ [\mathrm{MPa}],\ p = 1\,000\ [\mathrm{MPa}].$$

Fig. 3 shows that Fourier series expansion is not able to fairly approximate the hyperbolic course obtained from the FEM analysis. The ability of approximation remains approximately the same even when summation parameter P in (7) is increased from $P = 2$ up to $P = 5$. The increasing of computational time associated with the increasing of parameter P does not significantly improve results accuracy. Results obtained for these choices of P vary from the FEM results by about 15–30 %.

Figures Fig. 3 and Fig. 4 also show how the results are affected by the division of the coordinate intervals in numerical integrations: compare results tagged Fourier series expansion, $P = 2$, and results tagged Fourier series expansion, $P = 2$, finer interval division. The second mentioned course is obtained by using ten times finer division of the coordinate intervals. The results are a bit closer to FEM results but at the cost of a large increase in computational time.

Near both ends of the tube, there are obvious areas affected by the boundary conditions (displacement fixation).

2.3. Deformation Analysis, Fourier Taylor Series Expansion

The analysis with Fourier series expansion showed that the computational procedure with this series is quite time expensive due to working with large matrices when summation parameter P is increased and that this series expansion is not an ideal choice for a prediction of deformations of the isotropic tube subjected to internal pressure p.

Previous results indicate that it might be more appropriate to use a power series for displacement functions approximation but it is also desirable to maintain series expansion that is periodic in variable ξ^2. Therefore, the combination of Taylor and Fourier series expansion is used. Taylor series expansion is used for coordinates ξ^1 and ξ^3 while Fourier series expansion is used for coordinate ξ^2. This combination is named Fourier Taylor series expansion and subscript $_{FT}$ is

used for all variables when this new series expansion is used in the analysis. The semi-analytical method with Fourier Taylor series expansion can be hereafter abbreviated to SAFT for simplicity.

2.3.1. Displacement Functions

Fourier Taylor series expansion fulfilling the boundary conditions according to Fig. 1 has the form

$$\begin{aligned}
\overset{\xi}{u}_{1_{FT}} &= \frac{1}{\sqrt{\overline{s}}} \sum_{h=0}^{P_T} \sum_{k=-P_F}^{P_F} \sum_{m=0}^{P_T} D_1^{hkm} \xi^{1^h} \mathrm{e}^{\mathrm{i}k\xi^2} \xi^{3^m} \xi^3 (\xi^3 - l), \\
\overset{\xi}{u}_{2_{FT}} &= \frac{1}{\sqrt{\overline{s}}} \sum_{h=0}^{P_T} \sum_{k=-P_F}^{P_F} \sum_{m=0}^{P_T} D_2^{hkm} \xi^{1^h} \mathrm{e}^{\mathrm{i}k\xi^2} \xi^{3^m} \xi^3 (\xi^3 - l), \\
\overset{\xi}{u}_{3_{FT}} &= \frac{1}{\sqrt{\overline{s}}} \sum_{h=0}^{P_T} \sum_{k=-P_F}^{P_F} \sum_{m=0}^{P_T} D_3^{hkm} \xi^{1^h} \mathrm{e}^{\mathrm{i}k\xi^2} \xi^{3^m} \xi^3 (\xi^3 - l),
\end{aligned} \tag{36}$$

where added terms ξ^3 and $(\xi^3 - l)$ ensure fulfillment of the boundary conditions because these terms (and thereby also displacement functions $\overset{\xi}{u}_{i_{FT}}$) are equal to zero for $\xi^3 = 0$ and $\xi^3 = l$.

Summation parameter for Fourier series expansion is denoted P_F and for Taylor series expansion P_T because these parameters can have different values. Scalar product $\overline{s}$ in (36) is computed as

$$\overline{s} = \int_0^t \xi^{1^h} \xi^{1^a} \,\mathrm{d}\xi^1 \int_0^l \xi^{3^m} (\xi^3 - l) \xi^{3^c} (\xi^3 - l) \,\mathrm{d}\xi^3 \tag{37}$$

and it serves for Fourier Taylor series expansion normalization.

The deformation analysis procedure is the same as in the previous text and therefore it will not be repeated at this place. The only difference is that unknown displacement functions are approximated by Fourier Taylor series expansion.

2.3.2. Results

The semi-analytical method with Fourier Taylor series expansion is tested for choices $P_T = 2, 3, 4$ while P_F remains $P_F = 1$ to reduce computational time and sizes of the used matrices. Figures Fig. 5 and Fig. 6 clearly show that Fourier Taylor series expansion is much better for prediction of radial deformations than Fourier series expansion. Even for choice $P_T = 2$ the approximation of the hyperbolic course is highly accurate and also the computed deformations of the outer face are very close to the FEM results. The numerical values of deformations can be improved by using ten times finer division of the coordinate intervals. Differences in comparison with the FEM results are for $P_T = 2$ less than 10 % for the basic division of the coordinate intervals and the finer division brings an improvement of about 5 %, see Fig. 5.

2.4. Isotropic Tube, Finite Element Model

In order to compare results computed by using the semi-analytical method, the isotropic tube is modeled in the FEA software Abaqus as the 3D deformable solid and 8-node linear brick elements with reduced integration and hourglass control are used for this analysis. This model is discretized with eight elements in the radial direction to capture the variation of radial displacement through the section.

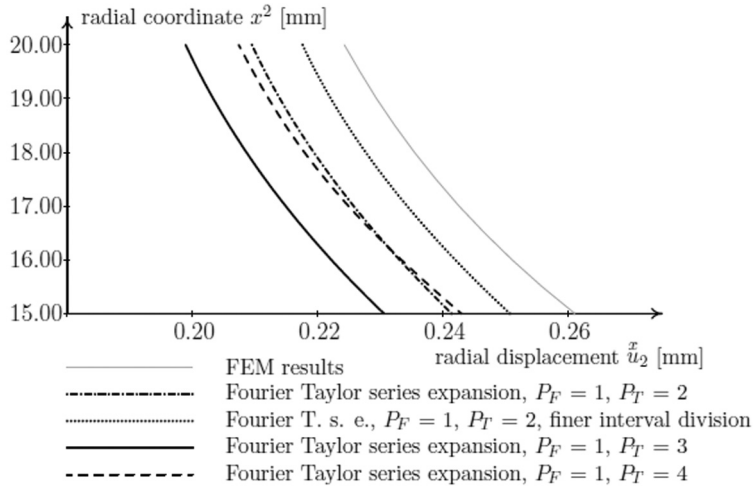

Fig. 5. Course of radial deformation evaluated at longitudinal coordinate $x^3 = l/2$, Fourier Taylor series expansion

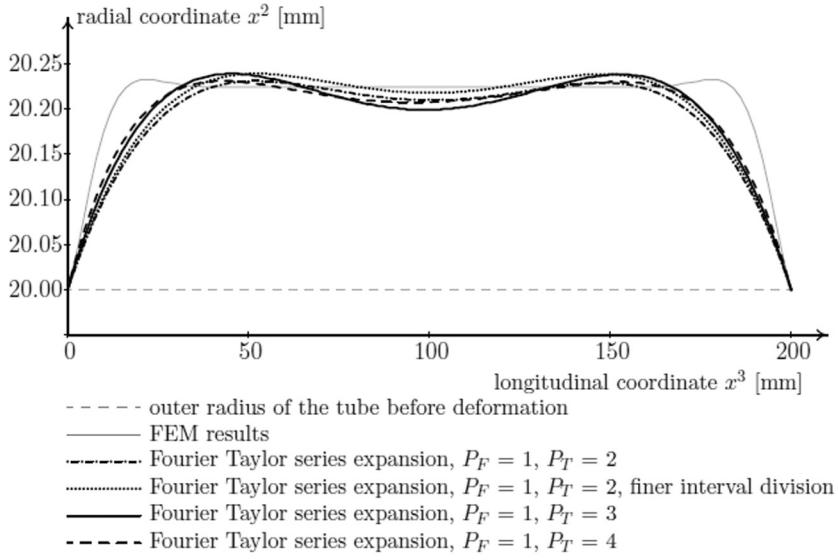

Fig. 6. Course of the outer face deformation, Fourier Taylor series expansion

3. Composite Tube under Internal Pressure

A composite material is included into analysis in this section. The main advantage of the method is in a geometry description and a material properties definition where Cartesian coordinate systems are used in combination with a curvilinear coordinate system. The tube with a circular cross section wound from a fiber composite is used for the procedure description because such simple geometry is easy to analyze also by using the finite element method.

The definition of anisotropic material properties is introduced and changes in the procedure are described in the first part of this section. To obtain the overall picture about the reliability of the semi-analytical method, analyses for ten different lay ups are performed and their results are compared with the FEM results.

3.1. Structure Description, Stiffness Matrix

Tubes are wound from the fiber composite in several layers and each layer is described by winding angle α (angle of fibers), see Fig. 7. There are four coordinate systems introduced for analysis purposes. Global Cartesian coordinate system, x^i, global circular coordinate system, ξ^i, local Cartesian coordinate system, μ^i, and local Cartesian coordinate system, ν^i, aligned with the direction of the local orthotrophy, see Fig. 7.

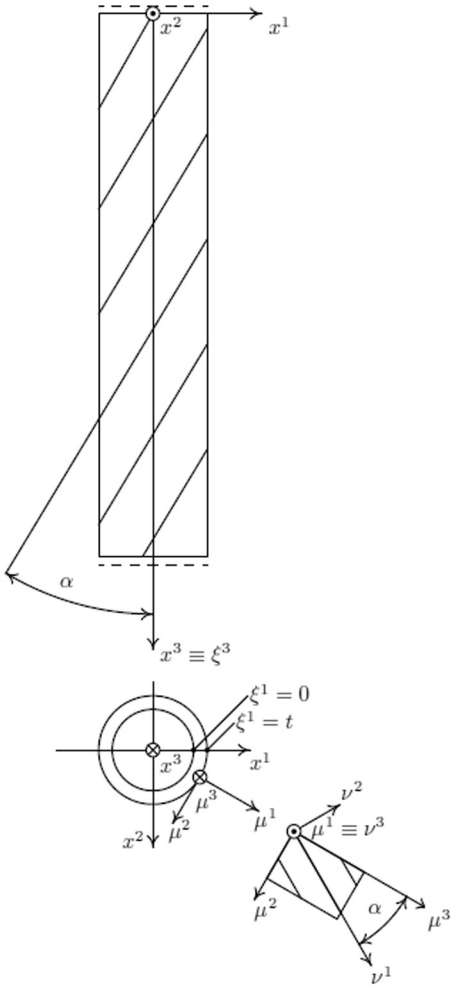

Fig. 7. Coordinate systems, composite tube

The importance and benefits of coordinate systems x^i (global Cartesian c. s.) and ξ^i (global circular c. s.) are described in the previous section and they are used in the anisotropic analysis in the similar way. Curvilinear coordinate system ξ^i is again used for the convenient geometry description and it significantly simplifies the limits of integration in numerical calculations. Global Cartesian coordinate system x^i serves for geometry representation and results plotting. However, in comparison with the isotropic case, it does not allow a correct description of anisotropic material properties.

Two new coordinate systems μ^i, ν^i are introduced for description of the material properties. Fig. 7 shows that local Cartesian coordinate system ν^i is aligned with the local orthotrophy. Axis ν^1 corresponds to the fiber direction, axis ν^2 is perpendicular to the fiber direction, and axis ν^3 represents the normal of a composite lay up. The coordinate system that is established in this way is commonly used for description of the material properties of composite materials.

In the analysis procedure, it is necessary to transform these material properties from coordinate system ν^i to global circular coordinate system ξ^i, and local coordinate system μ^i is introduced for this transformation. It is advantageous because transformations between ν^i and μ^i, μ^i and x^i, x^i and ξ^i, respectively, are very simple and they are defined in the following text.

The deformation analysis is the same as was described for the case when Fourier series expansion or Fourier Taylor series expansion are used for approximation of displacement functions. The only change is in the material properties of the structure.

Again, total potential energy is expressed in the form suitable for the numeric solution (SAF analysis)

$$\overset{\xi}{\Pi} = \frac{1}{2} A^{\mathrm{T}} \overset{\xi}{K} A - \overset{\xi}{P} A, \tag{38}$$

where stiffness matrix

$$\overset{\xi}{K} = \int_0^l \int_0^{2\pi} \int_0^t (B-G)^{\mathrm{T}} \overset{\xi}{E^{ijkl}} (B-G) \left| \overset{\xi}{g_{ij}} \right|^{\frac{1}{2}} \mathrm{d}\xi^1 \, \mathrm{d}\xi^2 \, \mathrm{d}\xi^3. \tag{39}$$

includes elasticity tensor $\overset{\nu}{E^{ijkl}}$ for the anisotropic material that is different from isotropic elasticity tensor $\overset{\xi}{E^{ijkl}_{iso}}$, see (23).

3.2. Elasticity Tensor of Anisotropic Material

Elasticity tensor $\overset{\nu}{E^{ijkl}}$ is known in local Cartesian coordinate system ν^i, which is aligned with the direction of the local orthotrophy. This elasticity tensor is transformed into global computational coordinate system ξ^i according to the rule

$$\overset{\xi}{E^{ijkl}} = \frac{\partial \xi^i}{\partial \nu^m} \frac{\partial \xi^j}{\partial \nu^n} \frac{\partial \xi^k}{\partial \nu^o} \frac{\partial \xi^l}{\partial \nu^p} \overset{\nu}{E^{mnop}} \tag{40}$$

with the transformation matrix

$$\frac{\partial \xi^i}{\partial \nu^j} = \frac{\partial \xi^i}{\partial x^k} \frac{\partial x^k}{\partial \mu^m} \frac{\partial \mu^m}{\partial \nu^j}, \tag{41}$$

where the transformation matrix $\partial \xi^i / \partial x^j$ is the inversion of term (4), transformation matrix $\partial x^i / \partial \mu^j$ is introduced by term (29), and the last transformation matrix

$$\frac{\partial \mu^i}{\partial \nu^j} = \begin{pmatrix} 0 & 0 & 1 \\ \sin\alpha & -\cos\alpha & 0 \\ \cos\alpha & \sin\alpha & 0 \end{pmatrix}. \tag{42}$$

Components of elasticity tensor (the full derivation of elasticity tensor is described in [12] and only the resulting form is shown at this place)

$$\overset{\nu}{E^{ijkl}} = \begin{pmatrix} \Phi_{1111} & 0 & 0 & 0 & \Phi_{1122} & 0 & 0 & 0 & \Phi_{1133} \\ 0 & G_{12} & 0 & G_{12} & 0 & 0 & 0 & 0 & 0 \\ 0 & 0 & G_{13} & 0 & 0 & 0 & G_{13} & 0 & 0 \\ 0 & G_{12} & 0 & G_{12} & 0 & 0 & 0 & 0 & 0 \\ \Phi_{2211} & 0 & 0 & 0 & \Phi_{2222} & 0 & 0 & 0 & \Phi_{2233} \\ 0 & 0 & 0 & 0 & 0 & G_{23} & 0 & G_{23} & 0 \\ 0 & 0 & G_{13} & 0 & 0 & 0 & G_{13} & 0 & 0 \\ 0 & 0 & 0 & 0 & 0 & G_{23} & 0 & G_{23} & 0 \\ \Phi_{3311} & 0 & 0 & 0 & \Phi_{3322} & 0 & 0 & 0 & \Phi_{3333} \end{pmatrix}, \tag{43}$$

where

$$\Phi_{1111} = \frac{1-\nu_{23}\nu_{32}}{N}E_{11}, \quad \Phi_{1122} = \frac{\nu_{21}+\nu_{23}\nu_{31}}{N}E_{11}, \quad \Phi_{1133} = \frac{\nu_{31}+\nu_{32}\nu_{21}}{N}E_{11},$$
$$\Phi_{2211} = \frac{\nu_{12}+\nu_{13}\nu_{32}}{N}E_{22}, \quad \Phi_{2222} = \frac{1-\nu_{13}\nu_{31}}{N}E_{22}, \quad \Phi_{2233} = \frac{\nu_{32}+\nu_{31}\nu_{12}}{N}E_{22},$$
$$\Phi_{3311} = \frac{\nu_{13}+\nu_{12}\nu_{23}}{N}E_{33}, \quad \Phi_{3322} = \frac{\nu_{23}+\nu_{21}\nu_{13}}{N}E_{33}, \quad \Phi_{3333} = \frac{1-\nu_{12}\nu_{21}}{N}E_{33}$$

with

$$N = 1-\nu_{12}\nu_{21}-\nu_{23}\nu_{32}-\nu_{31}\nu_{13}-\nu_{12}\nu_{23}\nu_{31}-\nu_{13}\nu_{32}\nu_{21}.$$

3.3. Material and Lay up Specification

Ten composite tubes with the same dimensions but with different lay ups are chosen for comprehensive comparative deformation analysis and their deformations are calculated and plotted.

All tubes have the same dimensions as the isotropic tube has in the previous section. Furthermore, the boundary conditions remain the same and they are apparent in Fig. 7. Nine tubes are wound in four layers and the orientation of fibers in each layer is defined by angle α, all layers have the same thickness 1.25 [mm]. One tube is wound in eight layers and all its layers have the thickness 0.625 [mm]. The layers are numbered from the inner layer to the outer.

Internal pressure $p = 100$ [MPa] is applied and five calculations are performed for each tube: the first three calculations with Fourier series expansion and summation parameter $P = 2$, $P = 3$, and $P = 5$, respectively, and the last two calculations with Fourier Taylor series expansion and summation parameters $P_T = 2$, and $P_T = 4$, respectively (with $P_F = 2$, see (36)).

As the first set, hypothetical tubes with the same winding angle in all layers are assumed and their deformations are analyzed. The first tube from this set has winding angle $\alpha = 0°$ (so that its all fibers are along the axial direction $x^3 = \xi^3$, see Fig. 7), the following tubes have winding angle α with the increment of $15°$, and the last one has winding angle $\alpha = 90°$ so that all its fibers are along the circumferential direction. Two additional tubes have a symmetric lay up and the last analyzed tube has non-symmetric lay up with the different fiber orientation in layers.

Using the generally known notation of a composite lay up, tubes have their stacking sequences as follow: $\alpha = [0°_4]$, $\alpha = [15°_4]$, $\alpha = [30°_4]$, $\alpha = [45°_4]$, $\alpha = [60°_4]$, $\alpha = [75°_4]$, $\alpha = [90°_4]$, $\alpha = [60°, -60°, -60°, 60°]$, $\alpha = [0°, 90°, 45°, -45°, -45°, 45°, 90°, 0°]$, $\alpha = [30°, 15°, -20°, 75°]$.

Material properties are described in local Cartesian coordinate system ν^i where axis ν^1 is aligned with the fiber direction, ν^2 is perpendicular to the fiber direction, and ν^3 is perpendicular to the plane of the lamina, see Fig. 7. Following material properties (carbon fibers T600 in an epoxy resin) are used in calculations — it means in elasticity tensor (43): $E_{11} = 127\,760$ [MPa], $E_{22} = E_{33} = 5\,066$ [MPa], $G_{12} = G_{13} = 3\,422$ [MPa], $G_{23} = E_{22}/(2(1+0.3))$, $\nu_{12} = 0.345$, $\nu_{23} = 0.3$, $\nu_{21} = \nu_{12}E_{22}/E_{11}$, $\nu_{31} = \nu_{13}E_{33}/E_{11}$, $\nu_{32} = \nu_{23}E_{33}/E_{22}$.

3.4. Composite Tube, Finite Element Model

The composite tubes are modeled as 3D deformable solids in the FEA software Abaqus, and 3D 20-node quadratic isoparametric elements with reduced integration are used for these linear elastic analyses. The models are divided into sections that correspond to the layers with a specific orientation, and each section has assigned the anisotropic material with appropriate orientation of material properties. All models are discretized with eight elements in radial direction to capture the variation of radial displacement through the sections.

For this simple circular tube, local cylindrical coordinate system (where 1, 2, and 3 directions refer to radial, circumferential, and axial directions, respectively) is used for the material properties definition in the finite element model. But when it is necessary to analyze more complex geometry with anisotropic material properties, the definition of correct material properties in different directions can be very laborious and complicated in the finite element model. For each element, it is required to ensure the definition of local coordinate system that allows the correct definition of anisotropic material properties.

In comparison, the semi-analytical method offers a clear and simple transition between curvilinear computational coordinate system while Cartesian coordinate system allows the unambiguous and comfortable definition of anisotropic material properties.

3.5. Results

Radial deformations are plotted in the similar way as for the isotropic tube. The only change is that courses for Fourier and Fourier Taylor series expansion are plotted in the same figure for better comparability.

Whole set of results is presented, see Fig. 8–18. Each figure contains the course of radial deformation $\overset{x}{u}_2$ through the wall (radial coordinate versus radial deformation) and course of the outer face deformation (radial coordinate after deformation versus longitudinal coordinate). From presented figures (radial coordinate versus radial deformation), it is obvious that course of radial deformation is strongly influenced by the composite lay up and the shape of this course significantly affects functioning of semi-analytical method.

Results obtained from the FEM analyses are used for comparison again. Differences between results from the semi-analytical analyses and from the FEM analysis are not expressed as a percentage because semi-analytical results are dependent on coordinates (radial coordinate x^2 and longitudinal coordinate x^3) in which they are evaluated. Discussed differences are sufficiently evident from plotted figures Fig. 8–18. The graphical representation of the results is probably the best way to get an overall idea how the semi-analytical method works.

All figures show that Fourier Taylor series expansion enables good approximation of course of the radial displacement. In most cases, satisfactory approximations are achieved with summation parameters $P_T = 2$, and $P_F = 2$. Calculations with these parameters are very fast and results are reliable. Fig. 11–12 show that summation parameter P_T should be increased to $P_T = 4$ for lay ups $\alpha = [45^\circ_4]$, $\alpha = [60^\circ_4]$ because using $P_T = 2$ does not provide good approximation.

In all anisotropic analyses, Fourier series expansion is not able to faithfully capture course of radial deformation through the wall thickness. This series expansion has only limited use when deformations of the outer face are investigated. Fig. 8–11, 15, and Fig. 17, respectively, demonstrate that Fourier series expansion provides good prediction of outer face deformations for lay ups specified in captions of these figures. But this series fails for the remaining cases.

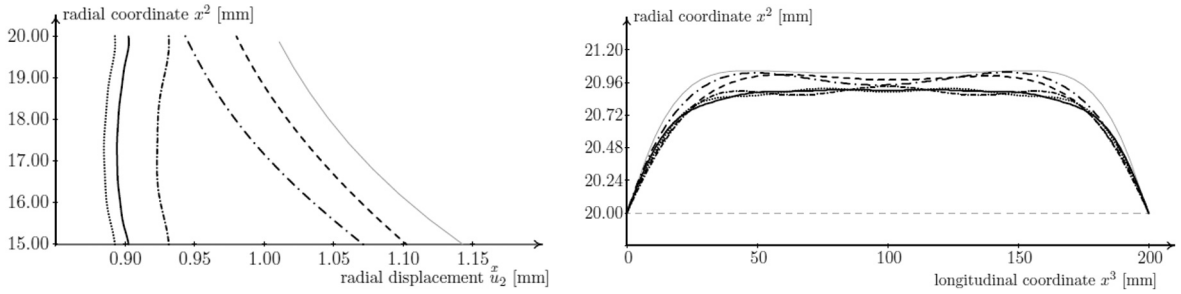

Fig. 8. Course of radial displacement, $\alpha = [0^\circ_4]$

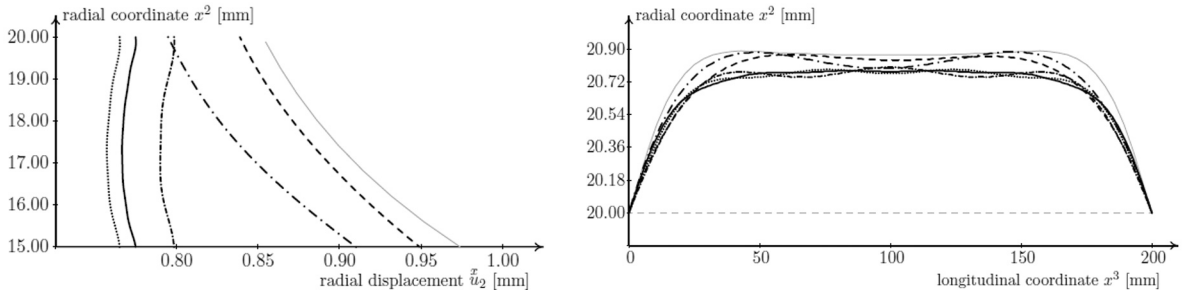

Fig. 9. Course of radial displacement, $\alpha = [15^\circ_4]$

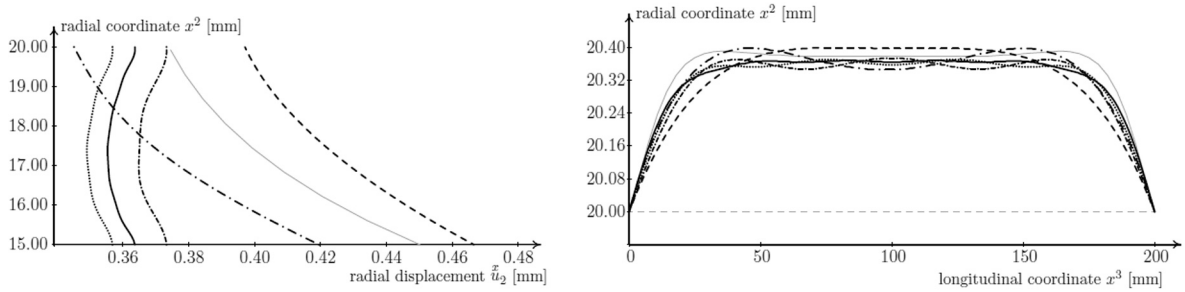

Fig. 10. Course of radial displacement, $\alpha = [30^\circ_4]$

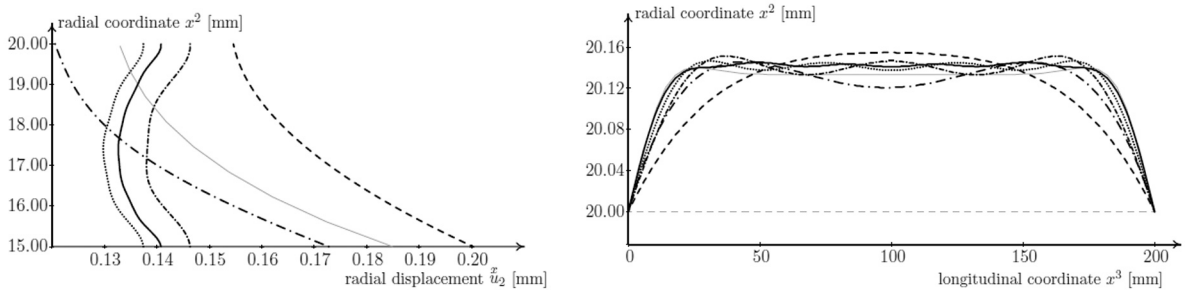

Fig. 11. Course of radial displacement, $\alpha = [45^\circ_4]$

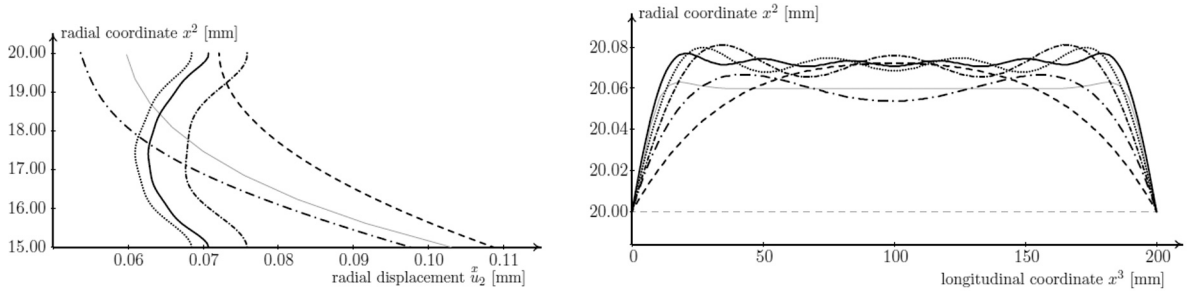

Fig. 12. Course of radial displacement, $\alpha = [60^\circ_4]$

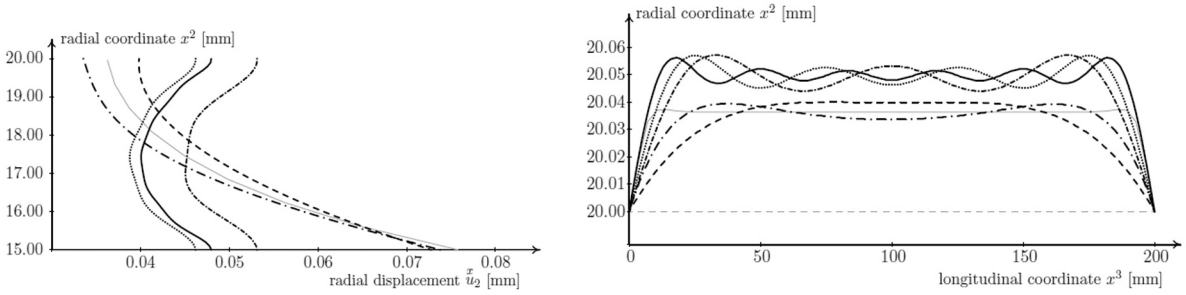

Fig. 13. Course of radial displacement, $\alpha = [75^\circ_4]$

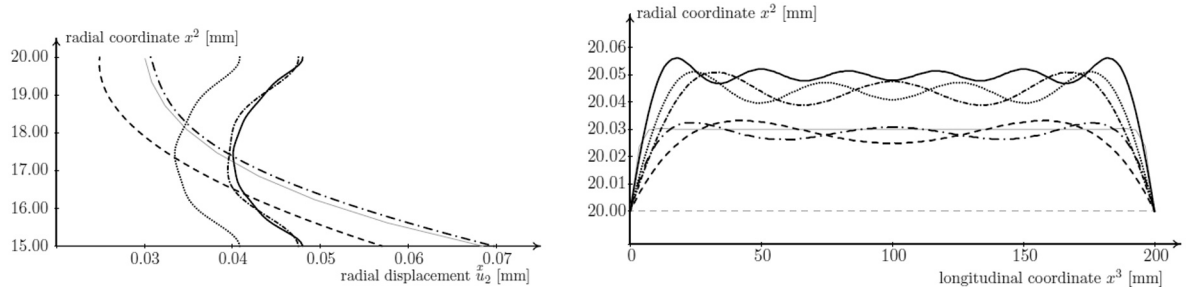

Fig. 14. Course of radial displacement, $\alpha = [90^\circ_4]$

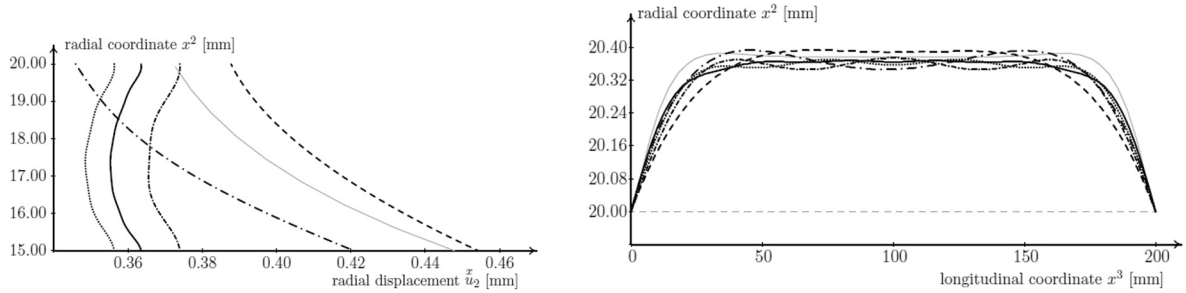

Fig. 15. Course of radial displacement, $\alpha = [60^\circ, -60^\circ, -60^\circ, 60^\circ]$

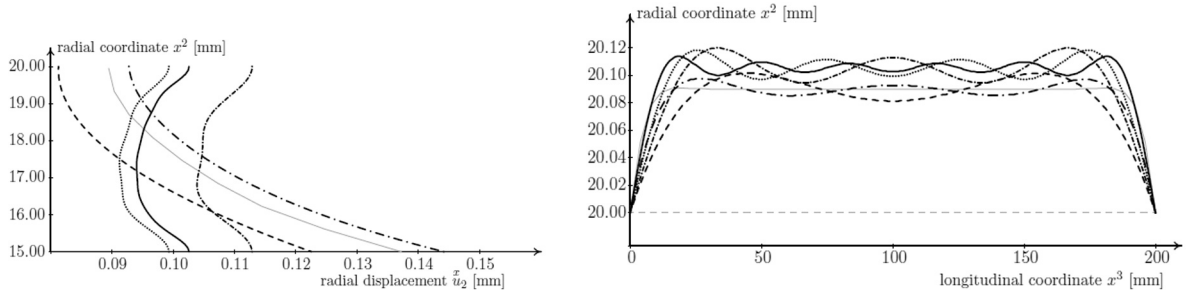

Fig. 16. Course of radial displacement, $\alpha = [0^\circ, 90^\circ, 45^\circ, -45^\circ, -45^\circ, 45^\circ, 90^\circ, 0^\circ]$

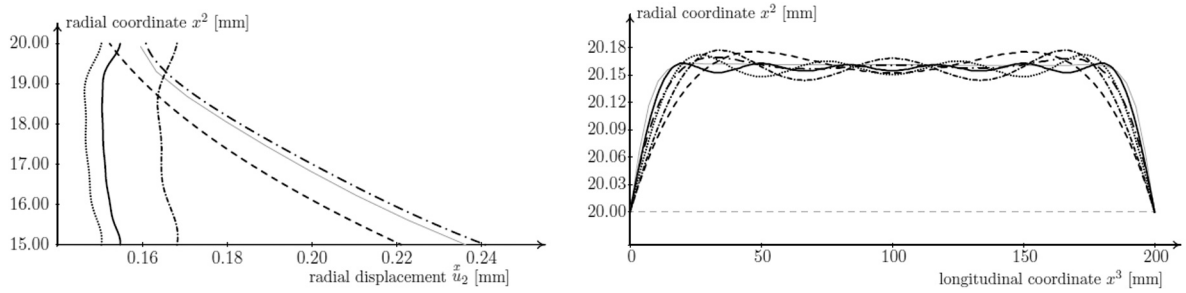

Fig. 17. Course of radial displacement, $\alpha = [30°, 15°, -20°, 75°]$

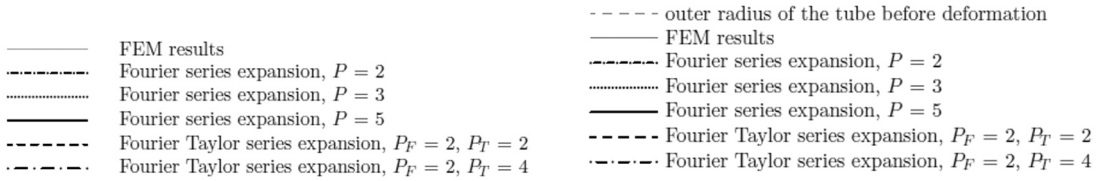

Fig. 18. Legend

4. Conclusion

The present article has described the semi-analytical method with Fourier and Fourier Taylor series and analytically tested simple isotropic and anisotropic structures. The different numbers of the series expansion members have been used and obtained results have been compared.

The main contribution and utility of this method is its versatility. Only one structure (a simple tube) under internal pressure load with only one type of boundary conditions (fixed ends) is presented in this work, but the semi-analytical method works also for any other load, geometry, or boundary conditions, without any simplistic assumptions. These possibilities are also briefly discussed in the text.

Courses of radial deformation are presented for the isotropic and composite tubes under internal pressure load. Only the graphical representation of the results is used because it is probably the best way to compare deformations computed by the semi-analytical method with the FEM results.

Deformations of the inner face have the same character as deformations of the outer face and therefore they are not plotted in figures. However, it should be mentioned that Fourier series does not capture changes in the tube thickness, while Fourier Taylor series does.

Presented results show that the semi-analytical method with Fourier Taylor series expansion provides precise approximation of the isotropic tubes deformations. The use of a power series enables satisfactory approximation of radial displacements. Furthermore, the shape of the outer face after deformation is predicted very well. Fourier Taylor series is also a good choice for predictions of deformations of anisotropic structures with a wide range of composite lay ups.

The use of Fourier series expansion in the semi-analytical method has significant limitations when analyses of structures under internal pressure load are performed. This series is not able to capture the course of radial deformation through the wall thickness and also its predictions of the outer face deformations are unreliable. This series can be involved into analysis in cases when for some reasons it is not possible to use Taylor series expansion. In such cases, however, it is necessary to calculate with limitations and risks that are presented in this article.

Acknowledgements

The authors would like to thank SGS 12/176/OHK2/3T/12.

Reference

[1] Akkus, N., Kawahara, M., Bending behaviors of thin composite pipes with reinforcing nodes, Material Science Research International 6 (2000) 131–135.

[2] Alderson, K. L., Evans, K. E., Failure mechanisms during the transverse loading of filament-wound pipes under static and low velocity impact conditions, Composites 23 (1992) 167–173.

[3] Brar, G. S., Hari, Y., Williams, D. K., Fourier serier analzsis of a cylindrical pressure vessel subjected to axial end load and external pressure, International Journal of Pressure Vessels and Piping 107 (2013) 27–37.

[4] Castro, S. G. P., Mittelstedt, Ch., Monteiro, F. A. C., Arbelo, A. M., Degenhardt, R., Ziegmann, G., A semi-analytical approach for linear and non-linear analysis of unstiffened laminated composite cylinders and cones under axial, torsion and pressure loads, Thin-Walled Structures 90 (2015) 61–73.

[5] Gal, D., Dvorkin, J., Stresses in anisotropic czlinders, Mechanics Research Communications 22 (1995) 109–113.

[6] Ganesan, N., Sivadas, K. R., Effect of coupling between in-plane strains and twist due to anisotropy on vibrations of composite shells, Computers and Structures 49 (1993) 481–493.

[7] Ghugal, Y. M., Shimpi, R. P., A review of refined shear deformation theories for isotropic and anisotropic laminated beams, Journal of reinforced Plastics and Composites 20 (2001) 255.

[8] Jamal, M., Lahlou, L., Midani, M., Zahrouni, H., Limam, A., Damil, N., Potier-Ferry, M., A semi-analytical buckling analysis of imperfect cylindrical shells under axial compression, International Journal of Solids and Structures 40 (2003) 1 311–1 327.

[9] Jeffrey, A., Mathematic for engineers and scientists, 6th edition, Chapman and Hall/CRC, 2004.

[10] Kayra, A., Yavuzbalkan, E., Semi-analytical study of free vibration characteristics of shear deformable filament wound anisotropic shells of revolution, Journal of Sound and Vibration 319 (2009) 260–281.

[11] Lovelock, D., Rund, H., Tensors, differential forms, and variational principles, Dover Publications, Inc., New York, 1989.

[12] Mares, T., Curvilinear elasticity in biomechanics, 2008. Retrieved from http://fsh.fsid.cvut.cz/∼marestom/z/z/habilitace/text/CurvilinearBiomechanics.pdf

[13] Pinto Correia, I. F., Barbosa, J. I., Mota Soares, C. M., Mota Soares, C. A., A finite element semi-analytical model for laminated axisymmetric shells: statics, dynamics and buckling, Computers and Structures 76 (2000) 299–317.

[14] Rosenow, M. W. K., Wind angle effects in glass fiber-reinforced polyester filament wound pipes, Composites 15 (1984) 144–152.

[15] Shadmehri, F., Hoa, S. V., Hojjati, M., Buckling of conical composite shells, Composite Structures 94 (2012) 787–792.

[16] Smerdov, A. A., A computational study in optimum formulations of optimization problems on laminated cylindrical shells for buckling: I. shells under axial compression, Composites Science and Technology 60 (2000) 2 057–2 066.

[17] Tang, K. T., Mathematical methods for engineers and scientists 3: Fourier Analysis, Partial Differential Equations and Variational Methods, Springer, 2007.

[18] Tarn, J. Q., Wang, Y. M., Laminated composite tubes under extension, torsion, bending, shearing and pressuring: a state space approach, Int. J. Solids Structures 38 (2001) 9 053–9 075.

[19] Wild, P. M., Vickers, G. W., Analysis of the filament-wound cylindrical shells under combined centrifugal pressure and axial loading, Composites A 28 (1997) 47–55.

[20] Xi, Z. C., Yam, L. H., Leung, T. P., Semi-analytical study of free vibration of composite shells of revolution based on the Reissner-Mindlin assumption, International Journal of Solids and Structures 33 (1996) 851–863.

[21] Xia, M., Takayanagi, H., Kemmochi, K., Analysis of filament-wound sandwich pipe under internal pressure, Composite Structures 51 (2001) 273–283.

[22] Xia, M., Takayanagi, H., Kemmochi, K., Analysis of multi-layered filament-wound composite pipes under internal pressure, Composite Structures 53 (2001) 483–491.